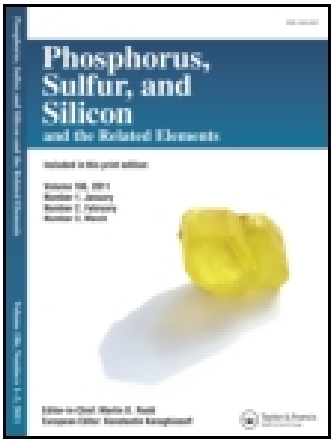

Phosphorus, Sulfur, and Silicon and the Related Elements
Publication details, including instructions for authors and subscription information:
http://www.tandfonline.com/loi/gpss20

Spectral Assignment of Phenanthrene Derivatives Based on 6H-Dibenzo[C,E][1,2] Oxaphosphinine 6-Oxide by NMR and Quantum Chemical Calculations

Sebastian Wagner [a], Muriel Rakotomalala [a], Frederick Chesneau [b], Thomas Zevaco [a] & Manfred Döring [a]

[a] Institute of Catalysis Research and Technology, Karlsruhe Institute of Technology, Eggenstein-Leopoldshafen, Germany

[b] Institute of Applied Physical Chemistry, University of Heidelberg, Heidelberg, Germany

Published online: 30 May 2012.

To cite this article: Sebastian Wagner, Muriel Rakotomalala, Frederick Chesneau, Thomas Zevaco & Manfred Döring (2012) Spectral Assignment of Phenanthrene Derivatives Based on 6H-Dibenzo[C,E][1,2] Oxaphosphinine 6-Oxide by NMR and Quantum Chemical Calculations, Phosphorus, Sulfur, and Silicon and the Related Elements, 187:7, 781-798, DOI: 10.1080/10426507.2011.610848

To link to this article: http://dx.doi.org/10.1080/10426507.2011.610848

Phosphorus, Sulfur, and Silicon, 187:781–798, 2012

ISSN: 1042-6507 print / 1563-5325 online
DOI: 10.1080/10426507.2011.610848

SPECTRAL ASSIGNMENT OF PHENANTHRENE DERIVATIVES BASED ON 6*H*-DIBENZO[*C,E*][1,2] OXAPHOSPHININE 6-OXIDE BY NMR AND QUANTUM CHEMICAL CALCULATIONS

Sebastian Wagner,[1] Muriel Rakotomalala,[1] Frederick Chesneau,[2] Thomas Zevaco,[1] and Manfred Döring[1]

[1]*Institute of Catalysis Research and Technology, Karlsruhe Institute of Technology, Eggenstein-Leopoldshafen, Germany*

[2]*Institute of Applied Physical Chemistry, University of Heidelberg, Heidelberg, Germany*

GRAPHICAL ABSTRACT

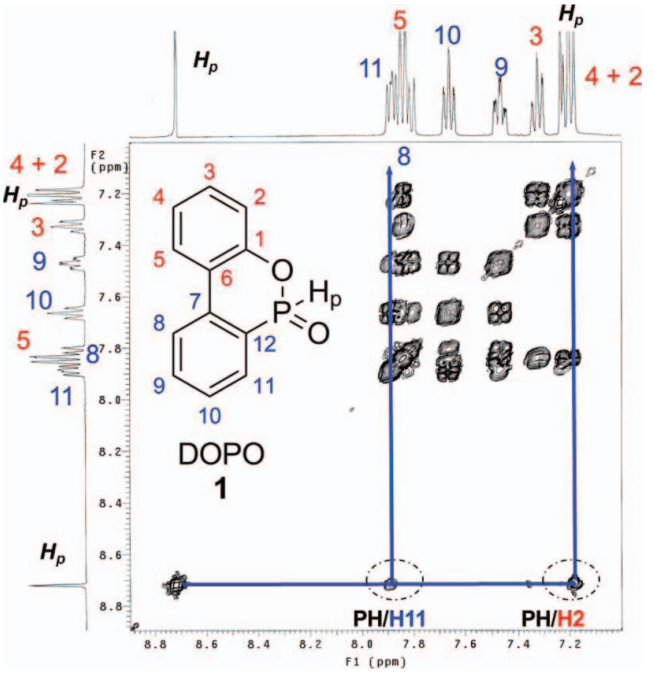

Abstract *Organophosphorus compounds such as 6H-dibenzo[c,e][1,2]oxaphosphinine 6-oxide (DOPO, **1**) and its derivatives are important and versatile compounds for a broad field*

Received 15 June 2011; accepted 1 August 2011.

DOPO (**1**) was kindly provided by Schill and Seilacher. The authors would also like to thank Mr. Zwick for measuring HR-MS, Ms. Schmelcher and Ms. Kölmel for elemental analysis, and Dr. Ingmar Held from Schill and Seilacher.

Address correspondence to Sebastian Wagner, Institute of Catalysis Research and Technology, Karlsruhe Institute of Technology, Hermann-von-Helmholtz Platz 1, 76344 Eggenstein-Leopoldshafen, Germany. E-mail: Sebastian.wagner@kit.edu

*of applications. However, a thorough spectral assignment is often subordinate to its chemical properties. This article presents and unambiguously attributes the ^{1}H and ^{13}C NMR spectra of DOPO (**1**), selected products yielded from the Atherton–Todd reaction (**2–4**), DOPO-HQ (**5**) as well as sulfur derivatives (**6–7**) via a set of 1D- and 2D-NMR experiments. The complex P-C and P-H coupling patterns are discussed and compared with the derivatives possessing different chemical environments around the phosphorus atom. In addition, we compared our results with density functional theory calculations. Even though the prediction of NMR data of organophosphorus compounds via molecular modeling is limited, this study presents a method that yields good results for this class of heterocycles. This knowledge should help to quickly assign NMR spectroscopic data of other DOPO (**1**) derivatives and can be extrapolated to organophosphorus compounds in general.*

Supplemental materials are available for this article. Go to the publisher's online edition of Phosphorus, Sulfur, and Silicon and the Related Elements *for the following free supplemental resource: NMR Spectra of Compounds 1-7 (Figures S1 - S15).*

Keywords NMR; DFT calculations; organophosphorus; heterocycles; Atherton–Todd reaction

INTRODUCTION

For several decades, organophosphorus molecules have been the subject of both academic and industrial research.[1–3] A wide range of applications have been reported in different areas of chemistry such as coordination chemistry, material science, homogeneous catalysis, development of biologically active compounds or pesticides, and additives for polymers such as lubricants or antioxidants.[4–10] There has recently been a growing interest from the flame retardant community regarding phosphorus-containing molecules as environmentally friendly alternatives to the existing, and often harmful, halogenated systems.[11–13] Among the broad range of documented phosphorus-based flame retardants, 6*H*-dibenzo[*c,e*][1,2]oxaphosphinine 6-oxide (DOPO, **1**, cf. Figure 1) and its derivatives were found to exhibit outstanding performance as flame retardants in various polymers such as polyesters, epoxies, and styrenics.[14,15]

In particular, epoxy resins, used for printed wiring boards, are rendered flame retardant by chemically linking DOPO (**1**) to the epoxy backbone (fusion process).[15] Despite the well-documented chemistry of DOPO (**1**) and its derivatives, the number of reports dealing with the detailed characterizations of these compounds is limited. Hence, the use of 1D- and 2D-NMR spectroscopic methods is still of interest.[16–18] Since the 1970s, a wide

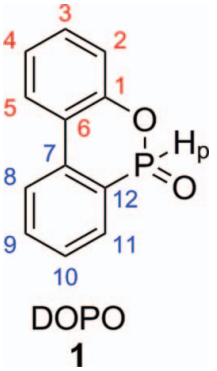

Figure 1 6*H*-dibenzo[*c,e*][1,2]oxaphosphinine 6-oxide (DOPO) (Color figure available online).

range of phosphorus compounds were characterized by NMR spectroscopy; however, in recent decades, industrially relevant phosphorus compounds such as DOPO (**1**) were not the subject of thorough spectroscopic investigations.[19] The present article attempts to fill this gap by comprehensively characterizing DOPO (**1**) via different NMR spectroscopy experiments. The attribution of the signals was compared to and supported by density functional theory (DFT) calculations using the individual gauge for localized orbitals (IGLO) method.[20,21] The attribution of NMR signals in organic molecules displaying conjugated and/or constrained ring systems is challenging. Over the last decade, significant effort has been invested in the understanding of NMR spectra via molecular modeling.[22] The calculation of nuclear shielding constants and spin-spin couplings requires optimized methods and basis sets.[23] Procedures involving localized orbital models such as LORG (localized orbital, local origin), IGLO, and GIAO (gauge inclusive atomic orbital), and the more modern CSGT method (continuous set of gauge transformations method) have been reported in the literature.[24–26]

In order to increase our understanding of the attributions and long-range couplings found in the DOPO (**1**) spectra, this study was extended to a range of derivatives generated from the Atherton–Todd reaction of DOPO (**1**) with resorcinol, phenol, and isopropanol. Hence, compounds **2**, **3**, and **4** were synthesized (Scheme 1). Even though those molecules were reported in the patent literature, their synthesis was not described in all cases. Hence, we introduce a new synthetic pathway starting from the commercially available DOPO (**1**) molecule.[27–29] The Atherton–Todd reaction is a well-known and easily applicable organophosphorus reaction.[30–32] Atherton and Todd[30] originally reported the reaction as a very effective tool to yield phosphoramidates. However, the reaction is described to be poor when alcohols are used as nucleophiles. Recent literature indicates that successful application of alcohols in the Atherton–Todd reaction is strongly dependent on the phosphorus species.[30,32] DOPO (**1**) in general was found to react easily with all kinds of nucleophiles under Atherton–Todd conditions. The characterization of these comparable molecules should support the proposed attribution and coupling pattern of the DOPO (**1**) base structure.

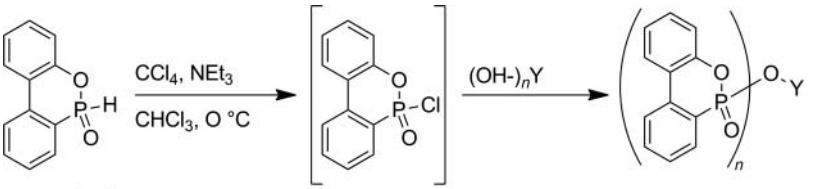

Scheme 1

Similarly, the known reaction product of DOPO (**1**) with hydroquinone (DOPO-HQ, **5**) was included in this study in order to correlate our results with the ones reported by Wang and co-workers.[33,34] In addition, we included two sulfur-containing DOPO derivatives recently reported by Rakotomalala and co-workers: DOPS (**6**) and its nucleophilic addition product to hydroquinone DOPS-HQ (**7**) to investigate the influence of the heteroatom

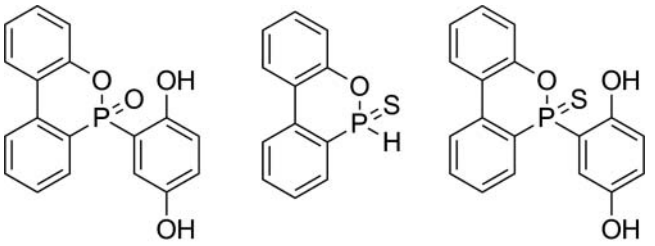

Figure 2 DOPO-HQ (5) and the sulfur derivatives DOPS (6) and DOPS-HQ (7).

present in the bridging dibenzooxaphosphinine ring on both chemical shifts and scalar couplings (Figure 2). [35]

It is known that an NMR-active nucleus, with a medium sensitivity, like phosphorus is able to generate coupling patterns with proton and carbon atoms over long distances. Up to ^{5}J couplings can be observed with a proper NMR resolution. P-H and P-C long-range couplings have been reported in the literature in systems based on phosphoramidates.[36] The attribution of the signals is complicated since the scalar coupling does not necessarily decrease with increasing distance from the phosphorus atom. The general structure of DOPO (**1**) and its derivatives exhibits an almost planar geometry with an extended conjugated system that favors the occurrence of long-range couplings.[37,38] Several models have been proposed to understand long-range spin-spin couplings in organophosphorus systems, ranging from hyperconjugative mechanisms to angle-dependant models involving P-C bonds and planes of the Pi-electron systems.[39,40] Thus, it was interesting to examine the P-H and P-C long-range couplings observed for DOPO (**1**) and its derivatives and compare them with the existing literature.

RESULTS AND DISCUSSION

As predicted, the deceptively simple ^{1}H NMR spectrum of DOPO (**1**) shows the presence of eight aromatic protons. The well-resolved signals in the aromatic region are indicative of a rigid ring system and coherent with the parent phenanthrene structure.[41,42] In addition, the doublet at 8.04 ppm ($^{1}J_{\text{P-H}} = 604$ Hz) is characteristic for the P-H bond. In the ^{1}H NMR spectrum, H2, H5, H8, and H11 are all expected to be doublets while H3, H4, H9, and H10 are expected to be doublets of doublets, which might appear in simple cases as triplets. However, in addition to two large doublets (7.84 and 7.23 ppm), a doublet of doublets (7.89 ppm) and two doublets of triplets (7.66 and 7.47 ppm) are observed.

The overlapping multiplets at lower field rendered the assignment cumbersome. Hence, the use of high-resolution 2D-NMR methods provided valuable complementary information for the assignment of the ^{1}H-NMR spectrum of DOPO (**1**).

As seen in Figure 1, DOPO (**1**) has two electronically distinct ring systems, i.e., two independent spin systems (H2-H5 and H8-H11). The standard COSY spectrum of DOPO (**1**) provided the first handle toward an assignment of the ^{1}H NMR data. Indeed, as seen in Figure 3, a correlation is observed between H_p and H11. The gCOSY spectrum emphasizes the correlation between H11 and H10 (Figure 4). As seen in Table 1, the coupling constant observed coincides with two neighboring protons on an ortho-substituted benzene ring

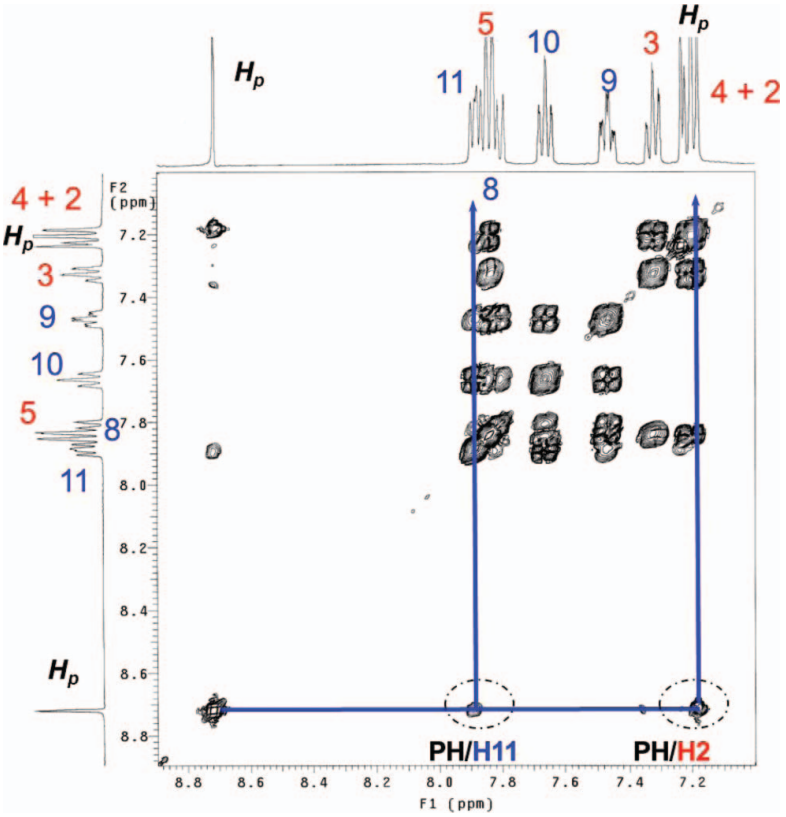

Figure 3 H,H-COSY NMR spectrum of 1 (DOPO). The H_p coupling with H2 and H11 is highlighted (Color figure available online).

with an electron withdrawing substituent. The ortho substitution is further confirmed as the triplet of doublets at 7.66 ppm (H10) is coupled to the triplet of doublets at 7.47 ppm (H9). The latter proton couples with the doublet of doublet at 7.81 ppm assigned to H8. The large coupling constants are indicative of a coupling with the phosphorus atom. In accordance with the electron withdrawing capability of the P = O moiety, the phosphorylated ring is

Table 1 ^{1}H NMR data of compound 1 (DOPO) in $CDCl_3$

	Experimental			
	δ (ppm)	J ^{1}Hx-^{1}Hy ^{3}J (Hz)		J ^{31}P-^{1}H (Hz)
H_p	8.04	—	—	604 (^{1}J)
H2	7.23 (d)	8.0	$^{3}J_{H2\text{-}H3}$	—
H3	7.33 (t)	8.3	$^{3}J_{H3\text{-}H2}$	1.0 (^{5}J)
H4	7.21 (t)	8.0	$^{3}J_{H4\text{-}H3}$	—
H5	7.84 (d)	7.6	$^{3}J_{H5\text{-}H4}$	—
H8	7.81 (dd)	7.6	$^{3}J_{H8\text{-}H9}$	16.5 (^{4}J)
H9	7.47 (td)	7.5	$^{3}J_{H9\text{-}H8}$	3.5 (^{5}J)
H10	7.66 (td)	8.3	$^{3}J_{H10\text{-}H9}$	1.0 (^{4}J)
H11	7.89 (d)	8.0	$^{3}J_{H11\text{-}H10}$	5.2 (^{3}J)

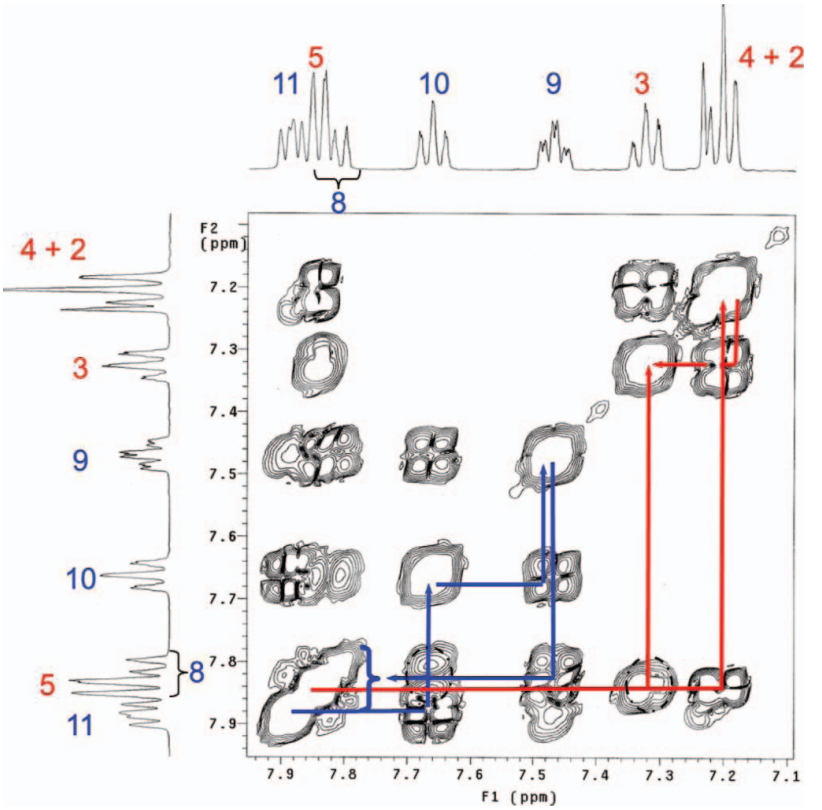

Figure 4 The gCOSY NMR spectrum of DOPO (1) (Color figure available online).

more downfield shifted (deshielded) than the oxygenated one. The standard COSY spectrum shown in Figure 3 emphasizes the long-range correlation between H_P and the peak observed at $\delta = 7.23$ ppm (d, $J = 8.00$ Hz). This provided a handle toward the assignment of the second ring system. The multiplicity indicates that the proton is ortho with respect to one of the two substituents on the phenyl ring (H2 or H5). However, a second doublet is observed at $\delta = 7.84$ ppm. The relative similarity in the electronic environment between H2 and H5 allowed the assignment of the doublet more deshielded to H5. Hence, this, and more importantly the correlation with H_p, led to the assigned of the second doublet to H2. This is coherent with the difference in the electron donating ability between phosphorus and oxygen. In DOPO (**1**), the high oxidation state of the phosphorus atom leads to a more deshielded H11 compared to H2. The gCOSY spectrum showed a correlation between H2 and the triplet at $\delta = 7.33$ ppm, which was assigned to H3. Consequently, H3 couples to a second triplet at 7.21 ppm (t, $J = 8.0$ Hz) associated with H4. A correlation between H4 and H5 is also observed in the H,H-COSY spectrum. Hence, all protons on the phenanthrene ring were assigned for DOPO (**1**). The observed NMR data are presented in Table 1.

The ^{13}C NMR of molecule **1** displays 12 signals, including eight methine carbons and four quaternary carbons. The correlations observed in the HMBC spectrum between H_P and two of the quaternary carbons enabled the assignment of C1 and C12 (Figure 5). Hence, the remaining quaternary carbons were assigned as C6 and C7. In addition, the correlations

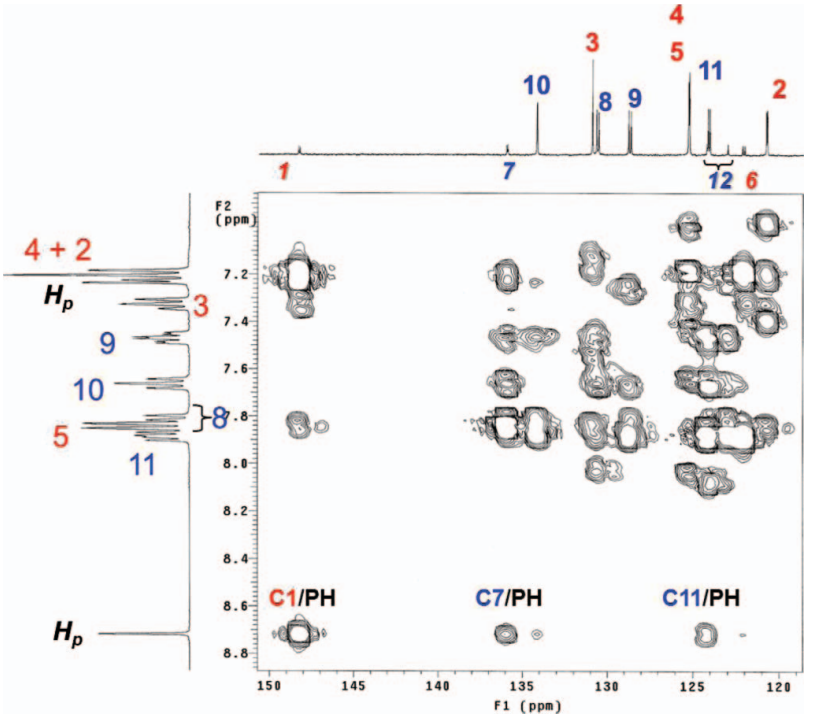

Figure 5 The HMBC spectrum of DOPO (1) showed H_p couplings with C1, C7, and C11 (Color figure available online).

observed in the HMQC spectrum of DOPO (**1**) enabled the unambiguous attribution of signals C2, C3, C4, C5, C8, C9, C10, and C11 (Figure 6).

The exact attribution of carbons C6 and C7 of the DOPO (**1**) structure is not straightforward and requires further proof. As seen in Figure 4, the signals attributed to the phosphorus-substituted ring systems are shifted more downfield than the signals associated with the oxygen-substituted ring system. Hence, of the remaining two unassigned quaternary carbons, the lower field signal ($\delta = 135.9$ ppm, $J_{P\text{-}C} = 6.5$ Hz) was attributed to C7 while the higher field signal ($\delta = 122.1$ ppm, $J_{P\text{-}C} = 12.3$ Hz) was assigned to C6. Supporting this assignment, C7 was the only carbon to be correlated to H_P in the long range HMBC spectrum of DOPO (**1**) (Figure 5). In addition, the HMBC spectrum reveals correlations between C7 and the protons H8, H9, H10, and H11 of the same ring system. From the other ring system, only a coupling for C7 with H5 was observed. Complementary to that observation, carbon C6 demonstrates couplings with all protons from its ring system (H2, H3, H4, and H5) and only with proton H8 from the opposite ring. Hence, we successfully assigned all carbon atoms. The ^{13}C NMR data of DOPO (**1**) are presented in Table 2.

MOLECULAR MODELING AND CHEMICAL SHIFTS CALCULATIONS

In order to support our results and propose some general guidelines for the attribution of NMR signals within such complex systems, the ^{1}H NMR and ^{13}C NMR spectrum of DOPO (**1**) was calculated using suitable DFT methods. Of different approaches, the VWN5 method and the NMR-specific IGLO-III basis set proved to be the most accurate.[43] The

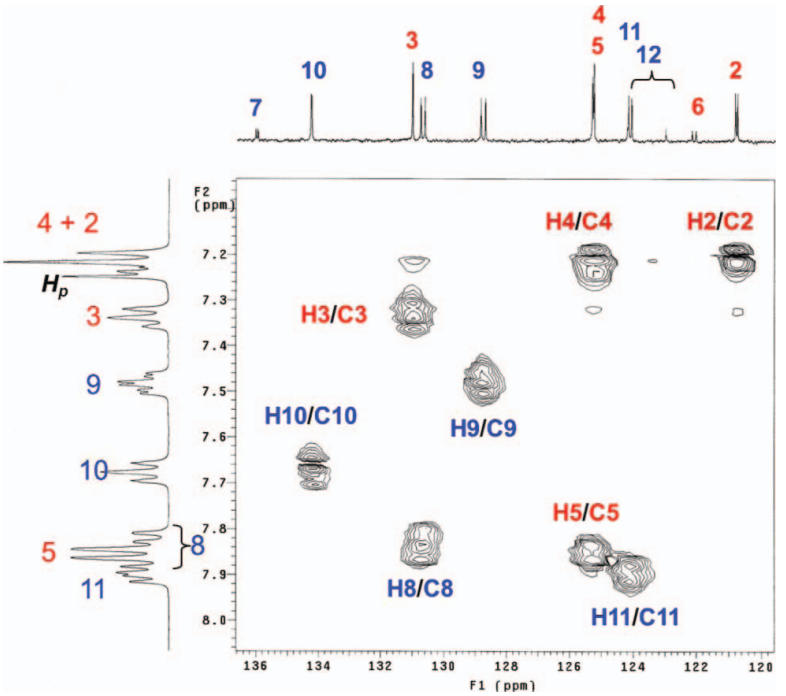

Figure 6 The HMQC spectrum of DOPO (1) (Color figure available online).

results of our calculations of the ^{1}H NMR chemical shifts of DOPO (**1**) in $CDCl_3$ are presented in Table 3.

The experimental and calculated chemical shifts are in good agreement at all levels of theory, except for protons H10 and H9, with an average unsigned error of 0.20 ppm for the B3LYP hybrid functional, 0.09 ppm for the mPW1PW hybrid functional, and 0.07 ppm for the VWN5 correlation functional (H9 and H10 were removed from error calculation, 0.14 ppm when H9 and H10 were included). These values are in line with the state of

Table 2 ^{13}C NMR data of 1 (DOPO)

#	δ (ppm)	J ^{31}P-^{13}C (Hz)
C1	148.2 (d)	8.4 (^{2}J)
C2	120.7 (d)	6.3 (^{3}J)
C3	131.0 (s)	
C4	125.3 (s)	
C5	125.2 (s)	
C6	122.1 (d)	12.2 (^{3}J)
C7	135.9 (d)	6.5 (^{2}J)
C8	130.7 (d)	12.7 (^{3}J)
C9	128.8 (d)	14.3 (^{4}J)
C10	134.2 (d)	2.4 (^{3}J)
C11	124.1 (d)	9.7 (^{2}J)
C12	123.6 (d)	122.1 (^{1}J)

Table 3 Calculated ^{1}H NMR chemical shifts of the ring protons of 1 (DOPO)

		VWN5		B3LYP			mPW1PW
#	Expt.	IGLO-III	Aug-cc-pVDZ	IGLO-III	Aug-cc-pVDZ	6311-G**	IGLO-III
H2	7.23	7.06	6.56	7.21	7.96	7.11	7.11
H3	7.33	7.46	7.26	7.51	8.96	8.01	7.61
H4	7.21	7.06	6.56	7.01	8.06	7.01	7.11
H5	7.84	7.86	7.96	8.01	9.46	8.01	8.01
H8	7.81	7.76	8.36	7.71	9.86	7.51	7.81
H9	7.47	7.76	8.06	7.81	9.46	8.21	7.91
H10	7.66	7.36	7.06	7.31	8.56	7.31	7.41
H11	7.89	7.86	7.16	8.11	8.96	8.01	7.91

Note: The experimental values are given for reference. All values are expressed in ppm.

the art.[44] Although the trends are coarsely reproduced, the more popular B3LYP/6311-G** level of theory fails to predict reasonable chemical shifts with an average unsigned error of 0.20 ppm, more than twice that of our most accurate method (VWN5/IGLO-III). Note that the double zeta method fails to quantitatively predict the chemical shifts both with VWN5 and B3LYP (average unsigned error: 0.35 and 1 ppm, respectively). Although it is a suitable method for organic molecules, our results suggest that it is not applicable for phosphorus-containing molecules such as DOPO (**1**). As seen in Table 3, the proton peaks for H10 and H9 are not correctly assigned in our calculations, irrespective of the functional or basis set used. To resolve this issue, we have calculated the ^{1}H NMR spectrum of phenylphosphinic acid both in $CDCl_3$ and in the gas phase and compared it with the values reported by Gervais et al.[45] As expected, on the basis of our experimental assignments, the chemical shifts of protons H10 and H9 are again inverted in these calculations (data not shown).

The chemical shift of the proton attached to the phosphorus was predicted to be 8.46 ppm using the VWN5 functional, 7.91 ppm using the mPW1PW functional (best agreement with our experiments), and 7.71 ppm using the B3LYP/6311G** method. In addition to the ^{1}H NMR, the ^{13}C NMR chemical shifts of DOPO (**1**) were calculated in the same manner and are summarized in Table 4.

Similar to the ^{1}H NMR calculations, the VWN5/IGLO-III method gave the best agreement with the experiment with an average unsigned error (C8–C11 excluded) of 1.3 ppm (mPW1PW: 1.6 ppm; B3LYP: 2.5 ppm). All methods used in this study give average unsigned errors in line with the state of the art.[46] However, the chemical shifts of carbons C8–C11 are wrongly predicted by all the methods used in this study. The error in the assignment of C9 and C10 can be correlated with that of their respective protons (H9 and H10, as described above). However, even though their respective protons are correctly assigned by our calculations, C8 and C11 are not. Our spectroscopic investigations clearly assign the peak at 130.7 ppm to C8 and that at 124.1 ppm to C11. In addition, our calculations also confirm some of the key carbons such as C1 and C12, as well as the hard to differentiate C6 and C7. To the best of our knowledge, our theoretical calculations of ^{13}C NMR chemical shifts are the first reported for organophosphorus compounds like **1**.

Even though the experimental assignments of the ^{1}H and ^{13}C NMR chemical shifts are largely reproduced by theory, especially for the oxygen-substituted ring, the method used (IGLO) showed limitations for the assignment of the proton and carbon atoms of the

Table 4 Calculated ^{13}C NMR chemical shifts for the ring carbons of 1 (DOPO)

#	Expt.	VWN5 IGLO-III	B3LYP IGLO-III	B3LYP 6311-G**	mPW1PW IGLO-III
C1	148.2	152.2	154	152.1	151.9
C2	120.7	120.1	119.9	118.3	119.4
C3	131	131.3	131.2	133.6	131.9
C4	125.3	123.9	122.8	123.3	123.5
C5	125.2	125.0	124.8	125.9	125.6
C6	122.1	124.0	124.4	118.9	123.1
C7	135.9	137.9	140.0	136.2	138.7
C8	130.7	123.8	122.5	121.5	123.3
C9	128.8	134.7	133.6	136.1	135.0
C10	134.2	128.5	127.2	126.9	127.9
C11	124.1	130.3	132.5	132.1	131.9
C12	123.6	126.5	127.1	119.0	124.3

Note: The experimental values are given for reference. All values are expressed in ppm.

phosphorus-substituted ring. Although IGLO is known to perform worse in the case of systems with delocalized electrons, repeating the calculations of the proton chemical shifts using the GIAO method implemented in the GAUSSIAN03 software package (gas phase, data not shown) did not yield an improvement in the average unsigned error (0.13 vs. 0.07 ppm for our best method).[25,47] Furthermore, a similar assignment for the chemical shifts of protons H9 and H10 was found. However, the error in the chemical shifts was more systematic with the latter method. Using the projected augmented-wave approach, Gervais et al. correctly predicted the relative chemical shifts of H9 and H10 in phenylphosphinic acid.[45,48] Therefore, we conclude that both the IGLO and GIAO methods wrongly assign the protons meta and para to PHOO groups and care should be taken when using these methods for the calculation of chemical shifts in organophosphorus compounds. Unfortunately, the complete assignment of the experimental NMR spectra of organophosphorus compounds is complicated and time-consuming. In contrast, our calculations, using the VWN5/IGLO-III method, require less than 15 min of computing time on a 2 GHz Core Duo machine with 2 GB of RAM. We expect the computational cost to significantly decrease on more modern machines. As seen above, the VWN5/IGLO-III method yields reasonable chemical shifts for DOPO (**1**) at a low computational cost. Thus, this study serves as a benchmark for the rapid calculation of NMR spectra of organophosphorus compounds. Furthermore, it supports and accelerates the cumbersome structure solving process.

SYNTHESIS AND CHARACTERIZATION OF DOPO DERIVATIVES

Since the DOPO (**1**) attribution was complete, we initiated the synthesis of derivatives of DOPO (**1**) via the Atherton–Todd approach and investigated the influence of the chemical environment around the phosphorus on the spectroscopic properties of the resulting molecules. The reaction products of DOPO with resorcinol (**2**), phenol (**3**), and isopropanol (**4**) in the presence of triethylamine and carbon tetrachloride were obtained in good yields (Scheme 1). The in situ formation of the oxychloride intermediate **1a** can be observed via ^{31}P NMR ($\delta\ ^{31}P = 21.3$ ppm). **1a** can also be isolated. Other reactive species were reported or proposed in the literature.[49] In addition, novel sulfur-containing DOPO (**1**) derivatives

Table 5 ^{1}H-NMR data of compound 1 (DOPO) and its derivatives 2–7 in $CDCl_3$[33]

#	1	2	3	4	5[a]	6	7[a]
H2	7.23 (d)	7.13 (tt)	7.20–7.15 (m)	7.14 (d)	7.25 (d)	7.21 (dd)	7.18 (dd)
H3	7.33 (t)	7.32 (m)	7.32–7.26 (m)	7.3 (t)	7.40 (t)	7.35 (dt)	7.47–7.36 (m)
H4	7.21 (t)	7.23 (t)	7.23 (t)	7.18 (t)	7.25 (t)	7.24 (t)	7.24 (dt)
H5	7.84 (d)	7.94–7.87 (m)	7.94–7.88 (m)	7.89–7.84 (m)	8.18 (t)	7.82 (d)	8.11 (d)
H8	7.81 (dd)	7.94–7.87 (m)	7.95 (dd)	7.9 (dd)	7.55 (dd)	7.81 (dd)	7.47–7.36 (m)
H9	7.47 (td)	7.42 (td)	7.45 (td)	7.43 (td)	7.46 (td)	7.52 (td)	7.47–7.36 (m)
H10	7.66 (td)	7.68 (t)	7.68 (t)	7.62 (t)	7.69 (t)	7.66 (t)	7.63 (dt)
H11	7.89 (d)	7.94–7.87 (m)	7.94–7.88 (m)	7.89–7.84 (m)	8.20 (t)	7.94 (dd)	8.12–8.09 (m)

[a]Measured in DMSO-d_6. All values are expressed in ppm.

DOPS (**6**) and DOPS-HQ (**7**) recently reported by Rakotomalala and co-workers, as well as DOPO-HQ (**5**) described by Wang and co-workers were added to this study.[33,35] The ^{1}H NMR data of DOPO (**1**) and its derivatives are presented in Table 5. Selected ^{1}H and ^{13}C NMR spectra for compounds 1–7 are presented in the Supplemental Materials (Figures S 1–S 15).

The ^{13}C NMR data as well as the phosphorus shifts are shown in Tables 6 and 7, respectively. It should be noted that DOPO-HQ (**5**) and DOPS-HQ (**7**) are insoluble in chloroform and thus were measured in DMSO-d_6. The results are still comparable since only protons H8 and H11 slightly move to lower as well as higher field, respectively. This trend was observed for all DOPO (**1**) derivatives measured in DMSO-d_6 (data not shown). Being a bridged molecule with two DOPO (**1**) groups, **2** was expected to show the most complex ^{1}H NMR data, but with the knowledge gained from the DOPO (**1**) attribution, the proton and carbon assignment was simplified (Figure 7, DMSO-d_6 was chosen due to a better resolution).

In addition, the attribution of **3** and **4** was successful and all results correlate with the attribution performed for the parent compound, DOPO (**1**). Our attribution of **5** correlates with the literature by Wang et al.[32] The DOPO (**1**) derivative **4** has the advantage that the isopropanol subunit has proton and carbon NMR signals in the aliphatic region. The HMBC

Table 6 ^{13}C NMR data of compound 1 (DOPO) and its derivatives 2–7 in $CDCl_3$[33]

#	1	2	3	4	5[a]	6	7[a]
C1	148.2 (d)	150.4 (d)	148.0 (d)	150.2 (d)	150.1 (d)	149.7 (d)	147.9 (d)
C2	120.7 (d)	120.5 (d)	119.3 (d)	120.3 (d)	120.5 (d)	120.8 (d)	121.0 (d)
C3	131.0 (s)	130.8 (s)	129.6 (s)	130.5 (s)	131.2 (s)	131.1 (s)	131.1 (s)
C4	125.3 (s)	125.3 (s)	124.5 (s)	124.7 (s)	124.4 (s)	124.9 (s)	125.1 (s)
C5	125.2 (s)	125.5 (s)	123.9 (s)	125.4 (s)	126.0 (s)	125.6 (s)	124.2 (d)
C6	122.1 (d)	122.6 (d)	121.4 (d)	122.9 (d)	121.8 (d)	123.6 (d)	122.5 (d)
C7	135.9 (d)	137.3 (d)	136.1 (d)	137.1 (d)	135.4 (d)	135.7 (d)	134.0 (d)
C8	130.7 (d)	131.0 (d)	129.7 (d)	130.2 (d)	130.8 (d)	131.7 (d)	130.1 (d)
C9	128.8 (d)	128.6 (d)	127.3 (d)	128.4 (d)	129.0 (d)	129.0 (d)	129.1 (d)
C10	134.2 (d)	134.2 (d)	132.8 (d)	133.4 (d)	133.4 (s)	134.9 (d)	132.8 (s)
C11	124.1 (d)	124.4 (d)	123.1 (d)	124.2 (d)	124.2 (d)	124.2 (d)	126.1 (s)
C12	123.6 (d)	121.3 (d)	120.0 (d)	121.0 (d)	126.2 (d)	125.4 (d)	129.2 (d)

[a]Measured in DMSO-d_6. All values are expressed in ppm.

Table 7 ^{31}P NMR data of DOPO (1) and its derivatives 2–7 in $CDCl_3$[33]

#	1	2	3	4	5[a]	6	7[a]
P	15.7	7.8/7.7	7.95	10.3	19.6	57.1	70.8

[a]Measured in DMSO-d_6. All values are expressed in ppm.

spectrum of compound **4** supports the general attribution of the neighboring quaternary carbons C6 and C7. C6 has strong cross peaks with the protons H2, H4, and H5 (same ring system). In addition, carbon C7 has strong cross peaks with H8, H10, and H11 (same ring system). These observations are in accordance with the attribution of the DOPO (**1**) spectrum. Similar results were found for all derivatives, which indicate that the phosphorus environment only has a small influence on the ^{1}H and ^{13}C NMR shifts of the phenanthrene ring.

Interestingly, the ^{13}C NMR data remain almost unaffected. Carbon atom C12, directly connected to the phosphorus atom, shows only a small shift toward higher fields when the hydrogen atom in DOPO (**1**) is replaced by oxygen as a result of the increased electron density around the phosphorus (compounds **2**–**4**). The replacement of the hydrogen atom by a sp^2 carbon belonging to the electron withdrawing hydroquinone group in **5** and **7** results in a deshielding effect. The sulfur atom in compounds **6** and **7** with its diffused d-orbitals has an additional deshielding effect on the respective C12 carbon atoms. These effects are more pronounced in the ^{31}P NMR spectra, with sulfur derivatives **6** and **7** being

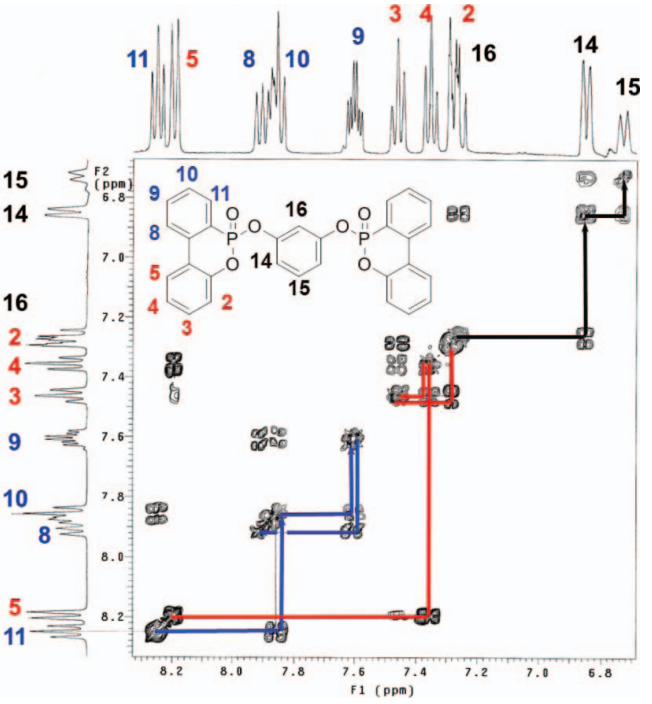

Figure 7 H,H-COSY NMR spectrum of **2** (Color figure available online).

strongly deshielded with respect to the oxygen containing derivatives. Due to the formation of diastereomers, **2** shows two signals in the ^{31}P NMR spectrum and a set of more complex multiplets in the ^{1}H NMR spectrum. The ^{13}C NMR spectrum remains almost unaffected.

CONCLUSION

The ^{1}H and ^{13}C NMR spectra of DOPO (**1**) were successfully assigned using a combination of 1D- and 2D-NMR techniques. The complete assignment of the protons on the dibenzooxaphosphinine ring was supported by molecular modeling calculations using DFT methods. The VWM5 method in combination with the IGLO-III basis set produced the most accurate predictions for the proton and carbon shifts of DOPO (**1**) in less than 15 min. Thus, this time-efficient model represents a useful tool for the structure solving process of organophosphorus molecules in general. The usefulness of this model was further confirmed as the assignment of ^{1}H and ^{13}C NMR spectra of DOPO (**1**) could be extrapolated on a series of substituted derivatives yielded from the Atherton–Todd reaction as well as thio-derivatives of DOPO (**1**). The variation of the phosphorus environment had only a slight impact on the ^{1}H and ^{13}C NMR data of the DOPO (**1**) derivatives. Since DOPO (**1**) and its derivatives are gaining more and more interest from academia and industry, the knowledge gained from this study can be applied toward the assignment of other polycyclic phosphorus compounds.

EXPERIMENTAL

General Experimental

Unless stated otherwise, solvents and chemicals were obtained from commercial sources and used without further purification. DOPO (**1**) was supplied by Schill and Seilacher. NMR experiments were performed on a Varian Inova-400 spectrometer (400 MHz), equipped with a 5-mm multinuclear, inverse detection z-gradient probe-head. The ^{1}H and ^{13}C NMR spectra were measured at 26 °C operating at 399.91 and 100.56 MHz, respectively. All samples were dissolved in 0.5 mL of $CDCl_3$ or DMSO-d_6. Chemical shifts are reported in ppm, and *J*-coupling constants are expressed in Hz. The calibration was performed using the remaining signal of the nondeuteriated part of the solvent (7.24 ppm) and the C-D characteristic coupling pattern of the deuteriated solvent in ^{13}C (77.0 ppm). The 2D spectra, H,C-HSQC, and H,C-HMBC were recorded using standard pulse sequences with z-gradients, as provided by Varian with the VNMR 6.1C control and processing software. The pulse conditions were as follows: for the ^{1}H NMR spectra, observation frequency is 399.912 MHz, acquisition time (at) = 3.744 s, number of scans (NS) = 16, number of dummy scans (SS) = 0, relaxation delay (d1) = 1.0 s, 90° pulse width = 6.4 μs, spectral width (sw) = 4799.0 Hz, no line broadening, and Fourier transform size (np) = 32K; for the ^{13}C NMR spectra, observation frequency is 100.56 MHz, aq = 1.20 s, ns = 1000, ss = 0, d1 = 1.0 s, 90° pulse width = 12.2 μs, sw = 21119.3 Hz, np = 32K, lb = 1.0 Hz; the H,H-COSY spectra were measured at 399.91 MHz and collected with 1K data points in F2 with 512 experiments 1 scan; the HSQC spectra were collected with 2k data points and spectral widths of 4000.0 Hz (F2) and 20,110.0 Hz, respectively; the HMBC spectra were obtained from 400 experiments 32 scans. The spectral widths used were the same as the HSQC experiment. The number of dummy scans was set to 32 and the delays were set to 5 Hz (long range Jnxh parameter) and 140 Hz (short range, J1xh parameter). All ^{31}P

NMR spectra are measured proton decoupled. All ^{13}C NMR spectra were measured proton decoupled and phosphorus coupled. ^{1}H NMR spectra were measured phosphorus coupled. Melting points are uncorrected and measured with a Büchi B-545. IR spectra were recorded with a Varian 660-IR (FT-IR). High-resolution mass spectrometry (HR MS) analyses were performed on a MicroMass GCT (time of flight [TOF]; electron ionization [EI], 70 eV). Elemental analysis was performed using a Vario EL III from Elementar Analysensystem GmbH.

Chemical Shift Calculations

All calculations were performed using the IGLO method implemented in the Orca 2.8 software package.[50] The geometry of the molecules was optimized at the RHF/PM3 level and refined at the B3LYP/6-31G* level of theory.[51–53] The chemical shifts were calculated using the VWN5 functional and IGLO-III basis set as well as the more popular B3LYP and mPW1PW functionals with either the Aug-cc-pVDZ or the 6-311G** basis sets.[54] All were used as implemented in the Orca 2.8 software package. The calculated values of δ were extracted using the following equation[55]:

$$\delta_{\text{calc}} = \sigma_{\text{ref}} - \sigma + \delta_{\text{ref}}$$

where δ_{ref} is the experimental chemical shift of the reference molecule, in our case benzene (^{1}H: $\delta = 7.36$ ppm, $\sigma = 22.7$ ppm; ^{13}C: $\delta = 128.5$ ppm, $\sigma = 38.55$ ppm), and σ_{ref} and σ are the calculated isotropic magnetic shielding values of the reference and molecule of interest, respectively.[55] We evaluated σ_{ref} to be 22.7 ± 0.1 ppm for ^{1}H and 38.55 ± 0.4 ppm for ^{13}C in the case of VWN5/IGLO-III. Benzene has been recommended for the calculation of chemical shifts of sp and sp^2 carbons.[55] When tetramethylsilane (TMS) was used as a reference, although the trends were reproduced, the calculated chemical shifts were shifted downfield by approximately 0.7 ppm. We have found benzene to be a better reference than TMS for our calculations. For all other methods, similar values of the isotropic magnetic shielding were obtained. To account for the solvent ($CDCl_3$), the COSMO model was used.[56] The values of 4.81 for the dielectric constant and 1.49 for the refractive index were applied. The PBE and B3LYP functional and the 6-31G(d) or 6-31+G(d,p) basis sets were used for the GIAO method implemented in the GAUSSIAN03 software package. Note on the computational cost: whereas the calculation of the ^{1}H and ^{13}C chemical shifts of DOPO using mPW1PW and B3LYP hybrid functionals with the IGLO-III basis set lasted 7–8 h on our hardware, VWN5 afforded more accurate chemical shift values for DOPO, with respect to experiment, in under 12 min. A typical calculation using the less accurate B3LYP/6311-G** method lasted approximately 1 h 20 min on the same hardware (Intel Core Duo 2 GHz, 2 GB RAM).

The synthesis of 6,6′-(1,3-phenylenebis(oxy))bis(6H-dibenzo[c,e][1,2]oxaphosphinine 6-oxide) **2** is given as a general example for an Atherton–Todd reaction. Compounds **3** and **4** are synthesized accordingly: A flame-dried, three-neck flask with a condenser, addition funnel, thermometer, and stirring bar was charged with 10.0 g (46.2 mmol) DOPO (**1**), 2.54 g (23.1 mmol) resorcinol, 7.65 g (50.0 mmol) carbon tetrachloride, and 70 mL of dry chloroform. The additional funnel was charged with 5.05 g (50.0 mmol) triethylamine diluted in 30 mL of dry chloroform. The triethylamine solution was added to the reaction mixture under vigorous stirring and the mixture was not allowed to

exceed 10 °C by cooling with an ice bath. The reaction progress was monitored by NMR spectroscopy. After 2 h, the reaction was complete and the mixture was washed three times with 100 mL brine. The combined organic phases were dried over sodium sulfate and then filtered over a short pad of alox (basic). The crude product was concentrated in vacuo yielding 10.76 g (20.1 mmol; 87%) of a white solid. mp: 150–152 °C; ^{31}P NMR (101 MHz, DMSO-d_6): 7.8 (s, 2P), 7.7 ppm (s, 2P); ^{1}H NMR (400 MHz, $CDCl_3$): 7.94–7.84 (m, 6H, H8/11/5), 7.86 (t, $J = 7.5$ Hz, 2H, H10), 7.42 (td, $J = 7.5$ Hz, $J_{P\text{-}H} = 3.6$ Hz, 2H, H9), 7.34–7.32 (m, 2H, H3), 7.23 (t, $J = 7.3$ Hz, 2H, H4), 7.13 (tt, $J = 8.0$ Hz, $J_{P\text{-}H} = 1.3$ Hz, 2H, H2), 7.12 (t, $J = 8.0$ Hz, 1H, H16), 6.84 (tt, $J = 8.1$ Hz, $J_{P\text{-}H} = 1.0$, 2H, H14), 6.72 ppm (d, $J_{P\text{-}H} = 1.3$ Hz, 1H, H15); ^{13}C NMR (100 MHz, $CDCl_3$) 150.4 (d, $J = 7.7$ Hz, 2C, C13), 149.9 (d, $J = 8.1$ Hz, 2C, C1), 137.3 (d, $J = 6.9$ Hz, 2C, C7), 134.2 (s, 2C, C10), 131.0 (s, 2C, C8), 130.8 (s, 2C, C3), 130.4 (s, 1C, C15), 128.6 (d, $J = 15{,}8$ Hz, 2C, C9), 125.5 (s, 2C, C5), 125.3 (s, 2C, C4), 124.4 (d, $J = 12{,}4$ Hz, 2C, C11), 122.6 (d, $J = 12.2$ Hz, 2C, C6), 121.3 (d, $J = 185$ Hz, 2C, C12), 120.5 (d, $J = 6.1$ Hz, 2C, C2), 117.7 (s, 2C, C14), 113.8 ppm (d, $J = 3.8$ Hz, 1C, C16); IR (KBr) $\tilde{\nu}$: 3110.9 (w, Ar-H), 3066.1 (w, Ar-H), 1594.9 (vs, C=C), 1558.9 (m, C=C), 1475.8 (vs, C=C), 1448.1 (w), 1430.6 (m, P-Ar), 1289.4 (s, P=O), 1273.5 (vs, P=O), 1243.4 (s, C−O), 1203.0 (m), 1132.6 (m), 1118.3 (s), 979.5 (s, P−O), 948.9 (vs, P−O), 907.1 (s), 793.1 (s), 748.5 (vs, C−H bend), 712.1 (m), 692.3 (m), 601.3 (w), 533.4 (s), 495.9 (m); HRMS (EI) calc. for [$^{12}C_{30}H_{20}P_2O_6$] 538.0735, found [$^{12}C_{30}H_{20}P_2O_6$] 538.0776; Anal. Calcd. For $^{12}C_{30}H_{20}P_2O_6$: C 66.92, H 3.74; found: C 66.97, H 3.86.

Synthesis of 6-phenoxy-6H-dibenzo[c,e][1,2]oxaphosphinine 6-oxide **3**: mp: 98 °C–102 °C; ^{31}P NMR (101 MHz; $CDCl_3$): 7.16 ppm (s, 1P); ^{1}H NMR (400 MHz, $CDCl_3$): 7.95 (dd, $J_{P\text{-}H} = 14.9$ Hz, $J = 7.5$ Hz, 1H, H8), 7.90–7.83 (m, 2H, H11/5), 7.62 (t, $J = 7.5$ Hz, 1H, H10), 7.42 (td, $J = 7.3$ Hz, $J_{P\text{-}H} = 3.6$ Hz, 1H, H9), 7.32–7.26 (m, 1H, H3), 7.23 (t, $J = 7.5$ Hz, 1H, H4), 7.20–7.12 (m, 4H, H2/15), 7.05 (t, $J = 7.6$ Hz, 1H, H16), 6.98–6.96 ppm (m, 2H, H14); ^{13}C NMR (100 MHz; $CDCl_3$) 148.9–148.6 (m, 2C, C12/13), 136.0 (d, $J = 7.1$ Hz, 1C, C7), 133.76 (d, $J = 2.5$ Hz, 1C, C10), 129.7 (d, $J = 9.3$ Hz, 1C, C8), 129.6 (s, 1C, C3), 128.6 (s, 2C, C15), 127.3 (d, $J = 15.8$ Hz, 1C, C9), 124.2 (s, 2C, C5/16), 123.9 (s, 1C, C4), 123.0 (d, $J = 12.4$ Hz, 1C, C11), 121.5 (d, $J = 12.5$ Hz, 1C, C6), 120.5 (d, $J = 177$ Hz, 1C, C12), 119.6–119.7 (m, 2C, C14), 119.2 ppm (d, $J = 6.9$ Hz, 1C, C2); IR (KBr) $\tilde{\nu}$: 3064 (w, Ar-H), 3019 (w, Ar-H), 2963 (w, R-H), 1609 (s, C=C), 1596 (m, C=C), 1488 (s, CH_2), 1477 (m, CH_2), 1430 (m, P-Ar), 1286, 1275 (vs, P=O), 1242 (s, C−O), 1196, 1169, 1078 (m, C−O), 1048, 1003, 973 (vs, P−O), 925 (vs, P−O), 796, 764 (m, C–H bend), 743, 729, 615, 536, 493 cm^{-1}; HRMS (EI) calc. for [$^{12}C_{18}H_{13}O_3{}^{31}P$] 308.0602, found [$^{12}C_{18}H_{15}O_3{}^{31}P$] 308.0572.

Synthesis of 6-isopropoxy-6*H*-dibenzo[*c,e*][1,2]oxaphosphinine 6-oxide **4**: mp: 107 °C–108 °C; ^{31}P NMR (101 MHz; DMSO-d_6): 9.74 ppm (s, 1P); ^{1}H NMR (400 MHz, $CDCl_3$): 7.90 (dd, $J_{P\text{-}H} = 16{,}3$ Hz, $J = 7{,}6$ Hz, 1H, H8), 7.89–7.84 (m, 2H, H11/5), 7.63 (t, $J = 7.3$ Hz, 1H, H10), 7.43 (td, $J = 7.3$ Hz, $J_{P\text{-}H} = 3.5$ Hz, 1H, H9), 7.30 (t, $J = 7.3$ Hz, 1H, H3), 7.18 (t, $J = 7.8$ Hz, 1H, H4), 7.15 (d, $J = 8.1$ Hz, 1H, H2) 4.86 (m, 1H, H13), 1.12 ppm (dd, $J_{P\text{-}H} = 9.5$ Hz, $J = 6.1$ Hz, 6H, H14); ^{13}C NMR (100 MHz, $CDCl_3$-d6): 150.2 (d, $J = 7.8$ Hz, 1C, C1), 137.1 (d, $J = 6.9$ Hz, 1C, C7), 133.4 (d, $J = 2.4$ Hz, 1C, C10), 130.5 (s, 1C, C3), 130.2 (d, $J = 9.2$ Hz, 1C, C8), 128.4 (d, $J = 15.4$ Hz, 1C, C9), 125.4 (s, 1C, C5), 124.7 (s, 1C, C4), 124.32 (d, $J = 12.1$ Hz, 1C, C11), 122.8 (d, $J = 12.1$ Hz, 1C, C6), 121.0 (d, $J = 190$ Hz, 1C, C12), 120.3 (d, $J = 6.5$ Hz, 1C, C2), 72.3 (d, $J = 6.7$ Hz, 1C, C13), 24.1–23.9 ppm (m, 2C, C14); IR (KBr) $\tilde{\nu}$: 3056 (w, Ar-H), 2979

(w, R-H), 1477 (m, CH_2), 1432 (m, P-Ar), 1386, 1275 (s, P═O), 1240 (s, C—O), 1204, 1157, 1099 (s, C—O), 1047, 973 (s, P—O), 920 (s, P—O), 795, 759 (m, C—H bend), 601, 551, 521 cm^{-1}; HRMS (EI) calc. for [$^{12}C_{15}H_{15}O_3{}^{31}P$] 274.0759, found [$^{12}C_{15}H_{15}O_3{}^{31}P$] 274.0691.

6-(2,5-dihydroxyphenyl)-6*H*-dibenzo[*c,e*][1,2]oxaphosphinine 6-oxide **5** was compared to the literature by Wang and co-workers.[33] The synthesis of 6H-dibenzo[*c,e*][1,2] oxaphosphinine 6-sulfide **6** and of 6-(2,5-dihydroxyphenyl)-6H-dibenzo[*c,e*][1,2]oxaphos phinine 6-sulfide **7** was performed as previously described by the authors.[35]

6-(2,5-dihydroxyphenyl)-6*H*-dibenzo[*c,e*][1,2]oxaphosphinine 6-oxide **(5):** ^{31}P NMR (101 MHz, DMSO-d_6) 19.6 ppm (s, 1P); ^1H NMR (400 MHz DMSO-d_6): 9.46 (s, 1H, H19), 8.22 (s, 1H, H20), 8.20 (dd, J = 8.2 Hz, J = 5.2 Hz, 1H, H11), 8.18 (dd, J = 7.8 Hz, J = 1.5 Hz, 1H, H5), 7.69 (t, J = 7.9 Hz, 1H, H10), 7.55 (dd, J = 14.4, J = 14.4, 1H, H8), 7.46 (dt, J = 7.5 Hz, J = 2.7 Hz, 1H, H9), 7.40 (t, J = 7.9 Hz, 1H, H3), 7.25 (t, J = 7.6 Hz, 1H, H3), 7.25 ppm (d, J = 8.0 Hz, 1H, H2); ^{13}C NMR (101 MHz, DMSO-d_6) 153.4 (d, J = 2.5 Hz, 1C, C17), 150.2 (s, 1C, C14), 150.1 (d, J = 4.2 Hz, 1C, C1), 135.4 (d, J = 5.4 Hz, 1C, C7), 133.4 (s, 1C, C10), 131.2 (s, 1C, C3), 130.8 (d, J = 12.3 Hz, 1C, C8), 129.0 (d, J = 12.9 Hz, 1C, C9), 126.3 (d, J = 129.5 Hz, 1C, C12), 126.0 (s, 1C, C5), 124.4 (s, 1C, C4), 124.2 (d, J = 9.3 Hz, 1C, C11), 123.3 (s, 1C, C16), 121.8 (d, J = 11.4 Hz, C6), 120.5 (d, J = 6.0 Hz, 1C, C2), 119.2 (d, J = 8.6 Hz, 1C, C16), 118.0 (d, J = 10.2 Hz, 1C, C15), 115.2 ppm (d, J = 142.6 Hz, 1C, C13).

6*H*-Dibenzo[*c*,*e*][1,2]oxaphosphinine 6-sulfide (**6**): mp: 88 °C; ^{31}P NMR (101 MHz, $CDCl_3$) 57.1 ppm (s, 1P); ^1H NMR (400 MHz, $CDCl_3$) 8.37 (d, J = 536.8 Hz, 1H, H_P), 7.95 (dd, J = 15.9 Hz, J = 7.6 Hz, 1H, H11), 7.8 (d, J = 8.1 Hz, 1H, H5), 7.81 (dd, J = 7.9 Hz, J = 5.1 Hz, 1H, H8), 7.66 (dt, J = 7.7 Hz, J = 1.1 Hz, 1H, H10), 7.52 (dt, J = 7.5 Hz, J = 3.2 Hz, 1H, H9), 7.35 (dt, J = 8.4 Hz, J = 1.1 Hz, 1H, H3), 7.24 (dt, J = 8.0 Hz, J = 0.8 Hz, 1H, H4), 7.21 ppm (dd, J = 8.1 Hz, J = 0.9 Hz, 1H, H2); ^{13}C NMR (101 MHz, $CDCl_3$) 149.7 (d, J = 11.2 Hz, 1C, C1), 135.7 (d, J = 5.4 Hz, 1C, C7), 134.9 (s, 1C, C10), 131.7 (d, J = 14.0 Hz, 1C, C8), 131.1 (s, 1C, C3), 129.0 (d, J = 14.7 Hz, 1C, C9), 125.6 (d, J = 5.2 Hz, 1C, C5), 125.4 (s, 1C, C12), 124.9 (d, J = 10.4 Hz, 1C, C2), 124.2 (d, J = 9.5 Hz, 1C,C11), 123.6 (d, J = 13.5 Hz, 1C, C6), 120.8 ppm (d, J = 5.9 Hz, 1C, C2).

2-(10-Thioxo-10*H*-9-oxa-10λ^5-phosphaphenanthren-10-yl) benzene-1,4-diol (**7**): mp.: 127 °C; ^{31}P NMR (101 MHz, DMSO-d_6) 73.6 ppm (s, 1P); ^1H NMR (400 MHz, DMSO-d_6) 9.53 (s, 1H, H19), 9.21 (s, 1H, H20), 8.11 (d, J = 7.8 Hz, 1H, H5), 8.12–8.09 (m, H11), 7.63 (dt, J = 6.6 Hz, J = 1.3 Hz, 1H, H10), 7.47–7.36 (m, 4H, H8, H9, H18, H3), 7.24 (dt, J = 7.2 Hz, J = 0.8 Hz, 1H, H4), 7.18 (dd, J = 8.1 Hz, J = 0.6 Hz, 1H, H2), 6.85 (dd, J = 8.7 Hz, J = 2.8 Hz, 1H, H16), 6.58 ppm (t, J = 5.6 Hz, 1H, H15); ^{13}C NMR (101 MHz, DMSO-d_6) 152.5 (s, 1C, C17), 150.0 (d, J = 18.2 Hz, 1C, C14), 149.7 (d, J = 9.8 Hz, 1C, C1), 134.0 (d, J = 4.6 Hz, 1C, C7), 132.8 (s, 1C, C10), 131.1 (s, 1C, C3), 130.1 (d, J = 14.2 Hz, 1C, C8), 129.2 (d, J = 106.4 Hz, 1C, C12), 129.2 (d, J = 14.6 Hz, 1C, C9), 126.1 (s, 1C, C11), 125.1 (s, 1C, C4), 124.2 (d, J = 8.8 Hz, 1C, C5), 123.4 (s, 1C, C16), 122.5 (d, J = 12.4 Hz, 1C, C6), 121.0 (d, J = 5.8 Hz, 1C, C2), 120.4 (d, J = 14.2 Hz, 1C, C18), 118.1 (d, J = 9.2 Hz, 1C, C15), 116.8 (d, J = 111.8 Hz, 1C, C13); IR (KBr) $\tilde{\nu}$: 3267 (br, -OH), 3190 (s, Ar-H), 1591 (s, P-Ar), 1580, 1471, 1221 (vs, P—O), 1182 (vs, P—O), 901 (vs, P = S), 752 cm^{-1}; HRMS (EI) calcd. for [$^{12}C_{18}H_{13}PO_3S$]$^+$ 340.0326, found 340.0323; Anal. Calcd. for $C_{18}H_{13}PO_3S$: C 63.52, H 3.85. Found: C 63.22, H 4.15.

REFERENCES

1. Quin, L. D. *A Guide to Organophosphorus Chemistry*; Wiley-Interscience, New York, 2000.
2. Westheimer, F. H. *Science* **1987,** 235, 1173-1178.
3. Cherkasov, R. A.; Kutyrev, G. A.; Pudovik, A. N. *Tetrahedron* **1985,** 41, 2567-2624.
4. Warner, V. D.; Mirth, D. B.; Dey, A. S. *J. Med. Chem.* **1973,** 16, 1185-1186.
5. Mevel, M.; Montier, T.; Lamarche, F.; Delépine, P.; Le Gall, T.; Yaouanc, J.-J.; Jaffrès, P.-A.; Cartier, D.; Lehn, P.; Clément, J.-C. *Bioconjugate Chem.* **2007,** 18, 1604-1611.
6. Levchik, S. V.; Weil, E. D. *Polym. Int.* **2005,** 54, 11-35.
7. Keglevich, G.; Kerenyi, A. *Trends Org. Chem.* **2008,** 12, 73-77.
8. Kollar, L.; Keglevich, G. *Chem. Rev.* **2010,** 110, 4257-4302.
9. Borch, R. F.; Canute, G. W. *J. Med. Chem.* **1991,** 34, 3044-3052.
10. Li, Z. R.; Han, J. Y.; Jiang, Y. Y.; Browne, P.; Knox, R. J.; Hu, L. Q. *Bioorgan. Med. Chem.* **2003,** 11, 4171-4178.
11. Levchik, S. V.; Weil, E. D. In: A. R. Horrocks, D. Price (Eds.), *Advances in Fire Retardant Materials*; Woodhead Publishing: Cambridge, 2008.
12. Weil, E. D.; Levchik, S. V. *J. Fire Sci.* **2004,** 22, 25-40.
13. Liu, W.; Varley, R. J.; Simon, G. P. *Polymer* **2007,** 48, 2345-2354.
14. Chang, S. J.; Chang, F. C. *J. Appl. Polym. Sci.* **1999,** 72, 109-122.
15. Rakotomalala, M.; Wagner, S.; Doering, M. *Materials* **2010,** 3, 4300-4327.
16. Vlad-Bubulac, T.; Hamciuc, C.; Serbezeanu, D. *Rev. Roum. Chim.* **2010,** 55, 667-672.
17. Ching, H. L.; Lin, H. T.; Sie, J. W.; Hwang, K. W.; Tu, A. P. *J. Poly. Sci. Part A: Poly. Chem.* **2010,** 20, 4555-4566.
18. Ching, H. L.; Lin, H. T.; Sheng, L. C.; Hann, J. H.; Yu, M. H.; Ya, R. T.; Wen, C. S. *Polymer* **2009,** 50, 2264-2272.
19. Nielsen, M. L.; Pustinger, J. V., Jr. *J. Phys. Chem.* **1964,** 68, 152-158.
20. Malkin, V. G.; Malkina, O. L.; Salahub, D. R. *Chem. Phys. Lett.* **1993,** 204, 87-95.
21. Krzysztof, W.; Hinton, J. F.; Pulay, P. *J. Am. Chem. Soc.* **1990,** 112, 8251-8260.
22. Pecul, M.; Urbanczyk, M.; Wodynski, A.; Jaszunski, M. *Magn. Reson. Chem.* **2011**. doi: 10.1002/mrc.2761
23. Aminova, R. A. *Chem. Comp. Sim. Butlerov Comm.* **2002,** 6, 11-30.
24. Hansen, A. E.; Bouman, T. D. *J. Chem. Phys.* **1985,** 82, 5035-5047.
25. Wolinski, K.; Hilton, J. F.; Pulay, P. *J. Am. Chem. Soc.* **1990,** 112, 8251-8260.
26. Cheeseman, J. R.; Trucks, G. W.; Keith, T. A.; Frisch, M. J. *J. Chem. Phys.* **1996,** 104, 5497-5509.
27. Kobayashi, J.; Ishikawa, A. *Jpn. Kokai Tokkoy Koho*, JP 2006083491 (2006).
28. Keglevich, G.; Kerenyi, A.; Mayer, B.; Kortvelyesi, T.; Ludanyi, K. *Transition Met. Chem.* **2008,** 33, 505-510.
29. Su, W. C.; Sheng, C. S. U.S. Patent, US 20050101793 (2005).
30. Atherton, F. R.; Todd, A. R. *J. Chem. Soc.* **1945**, 660-663.
31. Kannan, P.; Kishore, K. *Polymer* **1992,** 33, 412-422.
32. Wang, G.; Shen, R.; Xu, Q.; Goto, M.; Zhao, Y.; Han, L.-B. *J. Org. Chem.* **2010,** 72, 3890-3892.
33. Wang, C. S.; Shieh, J. Y. *Polymer* **1998,** 39, 5819-5826.
34. Wang, C. S.; Lee, M. C. *Polymer* **2000,** 41, 3631-3638.
35. Rakotomalala, M.; Wagner, S.; Zevaco, T.; Ciesielski, M.; Walter, O.; Doering, M. *Heterocycles* **2011,** 8, 743-753.
36. Gholivand, K.; Ghadimi, S.; Naderimanesh, H.; Forouzanfar, A. *Magn. Reson. Chem.* **2001,** 39, 684-688.
37. Hansen, P. E. *Org. Mag. Res.* **1978,** 11, 215-233.
38. Schaefer, A.; Seibold, S.; Lohstroh, W.; Walter, O.; Doering, M. *J. Appl. Polym. Sci.* **2007,** 105, 685-696.
39. Stone, E. W.; Maki, A. M. *Chem. Phys.* **1962,** 37, 1326-1333.
40. Griffin, C. E.; Gordon, M. *J. Am. Chem. Soc.* **1967,** 89, 4427-4431.

41. Ozubko, R. S.; Buchanan, G. W.; Smith, I. C. P. *Can. J. Chem.* **1974,** 52, 2493-2501.
42. Stothers, J. B.; Tan, C. T.; Wilson, N. K. *Organic Magn. Reson.* **1977,** 9, 408-413.
43. Vosko, S. H.; Wilk, L.; Nusair, M. *Can. J. Phys.* **1980,** 58, 1200-1211.
44. Jain, R.; Bally, T.; Rablen, P. R. *J. Org. Chem.* **2009,** 74, 4017-4023.
45. Gervais, C.; Coelho, C.; Azais, T.; Maquet, J.; Laurent, G.; Pourpoint, F.; Bonhomme, C.; Florian, P.; Alonso, B.; Guerrero, G.; Mutin, P. H.; Mauri, F. *J. Magn. Res.* **2007,** 187, 131-140.
46. Sarotti, A.; Pellegrinet, S. C. *J. Org. Chem.* **2009,** 74, 7254-7260.
47. Pople, J. A.; . *Gaussian 2004*; Gaussian, 03: Wallingford, 2004.
48. Pickard, C. J.; Mauri, F. *Phys. Rev. B* **2001,** 63, 245101-245113.
49. Georgiev, E. M.; Kaneti, J.; Troev, K.; Roundhill, D. M. *J. Am. Chem. Soc.* **1993,** 115, 10964-10973.
50. Schindler, M.; Kutzelnigg, W. *J. Chem. Phys.* **1982,** 76, 1919-1933.
51. Hehre, W. J.; Ditchfield, R.; Pople, J. A. *J. Chem. Phys.* **1972,** 56, 2257-2261.
52. Dill, J. D.; Pople, J. A. *J. Chem. Phys.* **1975,** 62, 2921-2923.
53. Francl, M. M.; Pietro, W. J.; Hehre, W. J.; Binkley, J. S.; Gordon, M. S.; DeFrees, D. J.; Pople, J. A. *J. Chem. Phys.* **1982,** 77, 3654-3665.
54. Kutzelnigg, W.; Fleischer, U.; Schindler, M. *The IGLO-Method: Ab Initio Calculation and Interpretation of NMR Chemical Shifts and Magnetic Susceptibilities*; Springer-Verlag: Heidelberg, 1990.
55. Sarotti, A. M.; Pellegrinet, S. C. *J. Org. Chem.* **2009,** 74, 7254-7260.
56. Klamt, A.; Schüürmann, G. *J. Chem. Soc. Perkin Trans.* **1993,** 5, 799-805.